Česká akademie věd
Ústav teorie informace a automatizace

Czech Academy of Sciences
Institute of Information Theory and Automation

RESEARCH REPORT

Petr Gebouský, Hana Křížová

Bayesian Identification from Incomplete Data with Application to Lymphedema Evaluation

No. 1991 September 2000

ÚTIA ČAV, P. O. Box 18, 182 08 Prague, Czech Republic
Fax: (+42)(2)6884903
E-mail: utia@utia.cas.cz

Bayesian Identification from Incomplete Data with Application to Lymphedema Evaluation *

Petr Gebouský[‡], Hana Křížová[△]
[‡]Department of Adaptive Systems, UTIA ČAV
[△]Department of Nuclear Medicine FNM
e-mail: gebousky@utia.cas.cz

September 7, 2000

Abstract

The Bayesian identification is one of possibilities how to gain model of real system from measured data. In this case it is employed for modeling of the accumulation of the radioactive tracer in local areas of upper limb on the basis of a sparse quantitative measurements during lymphoscintigraphic procedure. The main aim of selected compartmental model is the reconstruction of quantitative findings (whole time-activity curve) together with estimation of residence time on individual areas that can contribute to early and better diagnosis of the lymphedema.

Keywords: upper limb lymphedema, quantitative lymphoscintigraphy, modeling, Bayesian identification, incomplete data

1 Introduction

Lymphedema is a progressive condition characterized by four pathologic features: excess tissue protein, edema, chronic inflammation and fibrosis. It can be a primary condition but is more commonly secondary. Upper limb lymphedema is a frequent complication of breast cancer. According to Fruhling [1] the overall frequency of upper limb lymphedema is relatively high by patients with histologically proven breast cancer treated by unilateral surgery(22.5%). Surgery can be designated as one of the causal factors of upper limb lymphedema through interruption of the lymphatic flow in axillary level. Secondly, the role of radiation therapy has to be emphasized. This treatment technique approximately doubles the frequency of upper lymphedema.

*The project is supported by grants GA ČR 102/99/1564 and IGA MZ ČR 4581-2. The authors thank doctors of Department of Nuclear Medicine FNM for providing data and helpful comments.

Lymphedema is diagnosed in the majority of cases on the basis of clinical findings. Imaging studies permit objective confirmation of the diagnosis. A variety of imaging modalities have been employed in the evaluation of the lymphatic system.

Lymphoscintigraphy ([1], [5], [6]) has become the imaging modality of choice for evaluation of lymphatic system. It is a noninvasive technique in which radionuclides are used to image regional lymph drainage systems. Whereas qualitative lymphoscintigraphy allows the characterization of lymphatic morphology, quantitative clearance data were proved to be superior to qualitative image interpretation in detection of mild or incipient cases of lymphedema. However former quantitative methods showed good results just in detection of lower limb lymphedema, the identical methods are not suitable for evaluation of upper limb.

The full sequence of measurements necessary for quantitative lymphoscintigraphy in requisite time interval can be obtained in some academic studies only. Otherwise it rubs problem of time and money severity, health condition of patients is the other confining factor. Extremities are scanned in a few time moments at common investigation - the standard number ranges from 2 to 3 (in special cases 5). Then the commonly used quantitative lymphoscintigraphic method can not be used or have to be modified.

The goal of this study is to propose quantitative method which bridges the disadvantage of the lack of measurements and assists to improve the accuracy of diagnosis. Presented approach makes use of powerful tool of Bayesian identification for modeling of the radioactive tracer accumulation in local areas of upper limb. The results are estimated regional time-activity curves afterwards, that can take place of full sequence of measurements. The residence time proved to be the important parameter in other application of nuclear medicine ([2]) is tested here as a relevant parameter for assessment of upper limb lymphedema. Doctors' request to propose method which suffices with 2 measurements is the biggest obstacle for fruition of reasonable results.

2 Layout

Document is organized in following structure. Section 3 deals with obtaining of scintigraphic data and their interpretation. Used parts of decision-making theory appears in section 4. Section 5 contains detailed description of problem. Concrete modeling is decribed in section 6 and followed by theoretical solution of demanded tasks in section 7. Section 8 deals with tests and tuning of realized estimator; practical results are demonstrate in section 9. Document is ended by discussion over results in section 10.

3 Lymphoscintigraphy

Lymphoscintigraphy is a simple, versatile and nontraumatic imaging technique, which may be well suited for assessment of lymphatic function even in patients not accessible to radiographic lymphography. It provides information about lymph transportation, filtration and reticuloendothelial function.

Patients

A total of 20 patients participated in the study. All subjects were evaluated clinically and by lymphoscintigraphy. All of them had primary or secondary lymphedema of various grades on one upper limb at least.

Scintigraphic Imaging

This section describes standardized approach to lymphoscintigraphic procedure and data acquisition applied to series of patients.

Radicolloid

A sulfur microcolloid labeled with Tc-99m, provided from commercialized kit, has been used. Each dose contains on average 1.5 mCi (55 MBq) of the product in fixed volume of 0.2 ml.

Exploration Method

Images of upper limbs were obtained with a general electric LFOV gamma camera with a low energy collimator and then digitally stored. Data acquisition was similar in all patients. Imaging was performed as follows:

1. The doses never contain the same quantity of radiotracer. For this reason 1 frame of 60 seconds was obtained at the injection site immediately after subcutaneous administration in the first interdigital space of the microcolloid to measure the local radioactivity.

2. The gamma camera was then positioned over the regional (axillary) lymph nodes and upper limb. The acquisition of the frames of 60 seconds was performed in various time moments (at least two, one in first 60 minutes and then after 180 minutes). Unlike the standard dynamic studies, the sequential imaging in every minute is omitted. Since lymph flow in resting extremities is very slow, standardized exercise was performed during study (active opening and closing of the fist).

The images stored on the computer hard disk were retrieved for data analysis involving regions of interests (ROI's) defining the regional lymph nodes, the upper and lower halves of the extremity and background (Fig. 1). All gamma-camera data acquired were corrected for background but not for decay of Tc-99m (half-time of decay is 6 hours). The local activity for each region (integral counts

Figure 1: Example of scintigraphic image of hand with definitions of regions.

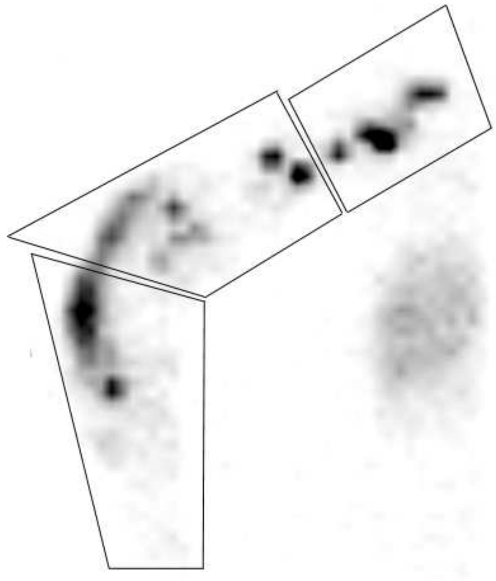

of pulses over ROI) was expressed as a percentage of the injected dose obtained from the first image.

The local initial activity at the injection site varies between 250000 - 450000 counts and activities on local regions of interests between 500 - 15000. Then the initial measurement at the injection site is certain (in relative coordinates) in comparison with data obtained later with respect of characteristics of the assumed Poisson distribution of measured activity expressed as counts of pulses.

Standard Interpretation

Lymphatic function is quantified in former studies by calculating dynamic parameters (appearance time, uptake after 2-5 hours according study). The appearance time measured on axillary nodes reflects the rapidity of lymphatic clearance. Uptake of radioactivity reflects the long time function of lymphatic system. Unfortunately this method that was verified on lower limbs revealed oneself as improper for assessing of upper limb lymphedema.

Qualitative image interpretation included evaluation of the injection site (number and size of lymph vessels), lymph collectors (number and size, collateral vessels, dermal backflow) and lymph nodes. With this qualitative interpretation alone, the diagnosis of lymphedema can be established only in higher grade of the disease.

As a result, both qualitative and quantitative studies should be performed simultaneously.

New Approach to Interpretation by Means of Modeling

Qualitative lymphoscintigraphy is a well described and offers good results but former performed studies indicated that quantitative clearance data are superior to qualitative image interpretation in detection mild or incipient cases of lymphedema. Hence we deal with quantitative lymphoscintigraphy in this paper above all.

The proposed method exploits only rare measurements (2-3) needful for qualitative image interpretation. Presented approach makes use of Bayesian identification for modeling of the radioactive tracer accumulation in defined regions of interests of upper limb (axillas, upper arm, forearm). The partial results are reconstructed regional time-activity curves afterwards. Lymphatic function is quantified here by parameter residence time. This parameter is defined as area under time-activity curve. There is also attempt to find moments of measurement that would be optimal for disposal in this method.

4 Methods

The Bayesian procedure used for the processing of image data is a specific case of exploitation of general theory described in [3] for the purpose of decision making.

Bayesian Decision-Making

Theory of statistical decision-making under uncertainty provides a unified logical structure for solving problems from parameter estimation, prediction, learning etc. up to feedback control. Bayesian approach rests on the fact that uncertainty has probability structure. It means that incomplete knowledge and randomness have the same operational consequences and should be treated in the same way — therefore Bayesian decision-making.

Static Design

The static decision making deals with the design and use of a single decision rule. The optimal selection of admissible rule can formulated on general level in this way:

Let's define decomposition of important elements called realization $\mathcal{Q} = (\mathcal{P}, a, \mathcal{F})$. Element $a \in a^*$ denotes direct decision of designer, $\mathcal{P} \in \mathcal{P}^*$ contains the knowledge available for decision (experience) and $\mathcal{F} \in \mathcal{F}^*$ contains the unavailable knowledge on the contrary (ignorance).

The aim of optimization is to select decision rule $\mathcal{R} : \mathcal{P}^* \to a^*$ that leads to the smallest value of the expected loss $E(\mathcal{Z})$. Expected loss assigns to the considered loss function $\mathcal{Z} : \mathcal{Q}^* \to [0, \infty]$ and decision rule a value that is independent of the realization uncertainty.

The optimal decision rule can be then constructed value-wise by assigning to each $\mathcal{P} \in \mathcal{P}^*$ a minimizing argument $a^o(\mathcal{P})$ in

$$\min_{a \in a^*} E\left[\mathcal{Z}(\mathcal{P}, a, \mathcal{F}) \,|\, \mathcal{P}, a\right]. \tag{1}$$

The probabilistic model $f(\mathcal{F}\,|\mathcal{P}, a\,)$ is needed for direct application of this basic optimization lemma.

Bayesian Identification

Bayesian identification([4]) is another part of decision-making theory. Its aim is not making decision but to create model, that the design works with afterwards.

Choice of System Model pertains to the first tasks of identification. Let us formulate hypothesis that our observation are described by a parameterized model

$$f\,(Y\,|U,\,\Theta\,) \tag{2}$$

where Y is a vector of observed output values y_i of system, Θ is vector of unknown parameters, U is a vector of observed (or known) input values u_i of system. Once the model structure is chosen or given, the problem of system identification is reduced to problem of parameter estimation.

Parameter Estimation The principle of Bayesian approach is to consider unknown Θ as a random vector to which a prior probability density function (pdf) $f\,(\Theta)$ is assigned, reflecting the prior knowledge about Θ. Considering an observation objective data Y, U, the subjective prior distribution can be corrected according to the Bayes rule

$$\begin{aligned} f(\Theta\,|Y,U\,) &= \frac{f(Y\,|U,\,\Theta\,)\ \overbrace{f(U\,|\Theta\,)}^{\substack{f(U) \\ \|}}\ f(\Theta)}{\int_{\Theta^*} f(Y\,|U,\,\Theta\,)\,f(U\,|\Theta\,)\,f(\Theta)d\Theta} = \\ &= \frac{f(Y\,|U,\,\Theta\,)\,f(\Theta)}{\int_{\Theta^*} f(Y\,|U,\,\Theta\,)\,f(\Theta)d\Theta} \propto f(Y\,|U,\,\Theta\,)\,f(\Theta) \end{aligned} \tag{3}$$

where Θ^* denotes set of possible values of quantity Θ and equality $f\,(U\,|\Theta\,) = f\,(U)$ expresses the assumption that the input signal is generated autonomly. This result is exploited further for e.g. prediction of output or estimation of unobservable variables.

The reason why just Bayesian identification was chosen for solving this problem is indicated below. The need for selecting prior pdf is often regarded as the main disadvantage of this approach but its use opens regular gate through which expert information can be introduced into learning in a systematic way. It bulks in this case when the amount of data at disposal is small. The information included in data is proportional to its amount at good experimental condition. Therefore information in data is relatively small and has to be complemented with additional information. Prior pdf offers among others a simple and clear way for introducing hard restrictions on parameters.

5 Problem Formulation

Consider a real system — lymphatic system in a limb — which is divided into 3 subsystems. They can be named after the position — regions of forearm, upper arm and axillas. On each subsystems the sequence of scalar outputs $y(\overline{t}) \equiv (y_1, y_2, \ldots, y_{\overline{t}})$ can be observed within lymphoscintigraphic procedure. The sequence of scalar inputs $u(\overline{t}) \equiv (u_1, u_2, \ldots, u_{\overline{t}})$ is known. It is injection of radiotracer which "excites" the system. Local outputs are not observed in each time moment but the sequence of outputs $y_o(N) \equiv (y_{t_1}, y_{t_2}, \ldots, y_{t_N})$ in time moments $t_o \equiv \{t_1, t_2, \ldots, t_N\}$, $N < \overline{t} < \infty$ is recorded only.

The main goal is design model which describes quantitatively real system in adequate way. The created model is utilized then for further tasks:

- Reconstruction of the whole time activity curve in each region from sparse measurements. The reason is that whole curve is more informative than a few points obtained from measurements and this curve can be and often is used for further processing.
- Estimation of the residence time in each region. Residence time is quantitative parameter proposed for assessment of lymphedema.
- Decision (optimization) when is the best time to measure to minimize an error at estimation of residence time. This task results from the necessity of limited number of data.

These points will be precisely mathematically formulated later.

6 Modeling

The injected radiotracer is carried by lymphatic flow to liver. The speed of the flow and radiotracer cumulation in time represents state of patient's lymphatic system. There are many possibilities how to describe this real system, therefore various models can be created.

Proposed model attempts to describe responses (cumulation) of patient during lymphoscintigraphy procedure in individual ROIs separately. The described systems are then simple SISO systems. The known input signal is injection of radiotracer. It is impulse where its size is obtained from first frame (see). The output signal is measured local activity expressed as percentage of the injected dose. We do not deal with more complicated modeling of response in the whole limb with spatial relations among regions in this paper.

6.1 Parameterized Model

The most important task of system identification is proper choice of parameterized model. Search for a compromise between the model quality and complexity of its treatment makes the model choice more art then science.

The model of lymphatic system function complies small piece of information about the problem. Assumptions are that inner behaviour of real system is dynamic deterministic t-invariant and the measurement is stochastic independent process. The individual response of patient in one ROI is modeled by a chain of simple identical compartmental models with a common unknown time constant, unknown gain and unknown number of constituents. Such parameterized model of d-order (order is equal to number of constituents) can be written:

$$\begin{aligned} x_t &= \sum_{i=1}^{d}(-1)^{i-1}\begin{pmatrix} d \\ i \end{pmatrix} a^i x_{t-i} + bu_t \\ y_t &= x_t + e_t \end{aligned} \tag{4}$$

where u is input, x inner deterministic variable of system and y its measurement with zero mean white Gaussian noise e. The noise can be interpreted as process noise or more precise the error of measurements. All unknown parameters — time constant a, total gain b, number of constituents d and variance of noise r respectively its inverse s (it is more convenient for calculations) — will be denoted Θ.

$$\Theta \equiv \{a,\, b,\, d,\, s \equiv \frac{1}{r}\} \tag{5}$$

The chosen 3-parameters models (omitting noise) was motivated by a standard modeling of distributed parameter systems. The model can seem primitive for good description of real system. The reason why this simple model is used is that it is impossible to estimate well many parameters from a few data. Therefore parameterized model contains only minimal number of parameters. Other more complicated (and possibly better) model could be applied in case of more data.

Assumed Poisson distribution of measurement noise was replaced in model by Gaussian distribution for the sake of feasibility. It does not make worse the model because Poisson distribution can be approximated by Gaussian on condition, that are fulfilled here (for $\lambda > 80$ $Po(\lambda) \approx \mathcal{N}(\lambda,\, \lambda)$).

The sequence of direct inputs $u(\overline{t})$ is known, it is unit impulse at time $t = 1$

$$u_1 = 1,\, u_2 = 0, \ldots,\, u_{\overline{t}} = 0. \tag{6}$$

The important assumption is that no radiotracer is present in body before injection, therefore initial conditions for inner variable x are zeros

$$x_0 = 0, \ldots,\, x_{-d} = 0. \tag{7}$$

Parameterized model (4) is transparent but not written in suitable way for our purposes. Therefore model is transformed to other form. It is advantageous to re-write all relations to matrix and vector form employing observation model (4) and initial conditions (7).

$$
\begin{bmatrix} 1 & a_1 & \dots & 0 & \dots \\ & 1 & a_1 & \dots & \ddots \\ & & & & \\ & & & \ddots & \ddots \\ 0 & & & & 1 \end{bmatrix}
\begin{bmatrix} x_{\bar{t}} \\ x_{\bar{t}-1} \\ \vdots \\ x_1 \end{bmatrix} = b \begin{bmatrix} u_{\bar{t}} \\ u_{\bar{t}-1} \\ \vdots \\ u_1 \end{bmatrix} \equiv A_{d,a}X = bU \Rightarrow \quad (8)
$$

$$
\Rightarrow X = bA_{d,a}^{-1}U
$$

$$
\begin{bmatrix} y_{t_N} \\ y_{t_{N-1}} \\ \vdots \\ y_{t_1} \end{bmatrix} = \begin{bmatrix} x_{t_N} \\ x_{t_{N-1}} \\ \vdots \\ x_{t_1} \end{bmatrix} + \begin{bmatrix} e_{t_N} \\ e_{t_{N-1}} \\ \vdots \\ e_{t_1} \end{bmatrix} \equiv Y_o = X_o + E_o \Rightarrow \tag{9}
$$

$$
\Rightarrow Y_o = bTA_{d,a}^{-1}U + E_o \quad = \quad b\widehat{Y}^*_{o;d,a} + E_o
$$

where coefficients a_i are determined by unknown a, d $\left(a_i = (-1)^i \begin{pmatrix} d \\ i \end{pmatrix} a^i\right)$, $\dim(X) = \dim(U) = \bar{t}$, b is scalar. Y_o denotes vector of recorded measurements, X_o vector of inner variable x in measurement moments and E_o is Gaussian noise $f(E_o) = \mathcal{N}_{E_o}\left(0, \frac{I}{s}\right)$, $\dim(Y_o) = \dim(X_o) = \dim(E_o) = N$ and T is $(N, \bar{t})$ permutation matrix.

The probability density function $f(Y_o\,|U, \Theta\,)$ is a form of parameterized model used in estimation

$$
\begin{aligned}
f(Y_o\,|U, \Theta\,) &= \mathcal{N}_{Y_o}\left(b\widehat{Y}^*_{o;d,a}, \frac{1}{s}I\right) = \\
&= \frac{s^{\frac{N}{2}}}{(2\pi)^{\frac{N}{2}}} \exp\left(-\frac{s}{2}\left(Y_o - b\widehat{Y}^*_{o;d,a}\right)^T \left(Y - b\widehat{Y}^*_{o;d,a}\right)\right)
\end{aligned} \tag{10}
$$

The unknown continuous parameter a enters the parametrized model in a very non-linear fashion and therefore it has to be disretised to get a feasible solution. Introduced indexes stress that for different a, d the matrix A alters.

6.2 Prior Information

Besides the model structure the information about parameters can be involved in the process of Bayesian learning. The known restrictions on model parameters is expressed in following table:

Parameter	Set of values	Description
a	$0 < a < 1$	stable nonoscilated models, interval can be tapered due to big time constant of process with respect to sampling period and order of model $(0.8 < a < 0,97)$
b	$0 < b < \overline{b}$	sign (input-output) preserved; the output during process has to be smaller than input impulse (dose)
d	$1 \leq d \leq \overline{d}$	upper limit is chosen big ($\overline{d} = 6$); the lower limit for more distant regions from injection site is better to set $1 < d$
$s = 1/r$	$s \geq 0$	variance is non-negative

The level of noise e which is described by parameter s is assumed to be similar for single regions at all patients. This noise is interpreted as error of measurement and the level of noise is similar for measurements of similar level. It ensues from assumed Poisson distribution of measured activity.

The group of suitable model orders d is supposed to be the similar for single regions at all patients too. The other parameters vary with each limb.

Prior information is involved in learning through prior pdf $f(\Theta)$. Applying the chain rule to joint prior distribution it can be written as product of conditional distributions:

$$f(\Theta) = f(a, b, d, s) = f(b|\, a, d, s)\, f(s)\, f(a, d) \tag{11}$$

Thinking it is no reason to distinguish prior distribution on s for different a, d (partial models) we define s as independent on a, d and the pdf $f(b|\, a, d, s)$ expresses demand on parameter b described in previous table. Joint pf $f(a, d)$ is defined as any arbitrary discrete distribution and the structures of pdfs are selected in conjugate form for the sake of feasibility ($f(b|\, a, d, s)$ - Gaussian, $f(s)$ - Wishart (gamma) distribution)

$$f(s) = \begin{cases} \frac{\left(\frac{1}{2}\epsilon\right)^{\frac{\delta+1}{2}}}{\Gamma\left(\frac{\delta+1}{2}\right)} s^{\frac{\delta-1}{2}} \exp\left(-\frac{s}{2}\epsilon\right) & \text{if } s > 0 \\ 0 & \text{if } s \leq 0 \end{cases} \tag{12}$$

$$f(b|\, a, d, s) = \mathcal{N}_b\left(\widehat{b}_{d,a}, \frac{1}{\rho_{d,a}^2 s}\right) = \frac{\rho_{d,a} s^{\frac{1}{2}}}{\sqrt{2\pi}} \exp\left(-\frac{\rho_{d,a}^2 s}{2}\left(b - \widehat{b}_{d,a}\right)^2\right) \tag{13}$$

where $\epsilon > 0$, $\delta > -1$, $\rho_{d,a} > 0$ and $\Gamma(\cdot)$ is Euler gamma function.

Assignment of values to parameters ϵ, δ, $\rho_{d,a}$, $\widehat{b}_{d,a}$ and stochastic matrix $f(a, d)$ completes the setting of prior distribution. The exponential discretisation of parameter a seems as the best choice because the behaviour of two systems with fix offset of time constant diverse more when the time constant comes near to instable area. Then stochastic matrix $f(a,\, d)$ is defined as uniform distribution. Distribution $f(s)$ can be expressed from expert knowledge (e.g. level of measurements, pre-apriori processing of data). Specification of $f(b|\, a,\, d,\, s)$ reflects the fact that we can never measure more quantity than we inject. Therefore it is found out $\overline{b}$ for each fix a, d, where maximum of the impulse response of the deterministic system is 1, and then is set $\widehat{b}_{d,a} = \frac{1}{2}\overline{b}$. This parameter can be better adjusted according to assumed average gain in single regions. Determination of parameter $\rho_{d,a}$ is more complicated and more approaches can be found too (e.g. use of quantiles). Gained experience showed that it is better to set this distribution flat.

6.3 Mathematical Description of Partial Tasks

Inner variable x_t represents the sought quantity. Sequence of values of this variable is defined as time-activity curve. Then tasks sequent to demanded goals and chosen model are as follows:

- estimation of model parameters $f(\Theta\, |y_o(N),\, u(\overline{t})\,)$.
- estimation of inner variable x_t between time moments $1 \leq t \leq \overline{t}$. Mean value $E\left(x_t\, |y_o(N),\, u(\overline{t})\right)$ and variance $\mathrm{var}\left(x_t\, |y_o(N),\, u(\overline{t})\right)$ are evaluated as sufficient results.
- estimation of area under time-activity curve $x(\overline{t})$ (residence time). The mean value and variance are the most important results.
- decision in which fix number of time moments is the best to measure output to minimize the error of residence time estimate (the concrete minimized loss function will be defined later).

All in the beginning roughly formulated goals are expressed exactly in mathematical terms now.

7 Theoretical Solution

Only final results are shown in this section. We make simplifications in letters $Y_o \equiv Y$.

7.1 Parameter Estimation

Bayesian estimator converts integral counts taken over regions of interest into posterior distribution of discretised common time constant, model order, gain and variance (respectively its inversion) of noise

$$f(\Theta\,|Y,U\,) \quad = \quad \frac{f(a,d)\rho_{d,a}s^{\frac{N+\delta}{2}}}{K}\exp\left\{-\frac{s}{2}\left[\left(Y-b\widehat{Y}^*_{d,a}\right)^T\left(Y-b\widehat{Y}^*_{d,a}\right)\right.\right. \quad (14)$$

$$+\epsilon + \rho_{d,a}^2 \left(b - \widehat{b}_{d,a}\right)^2 \Big] \Big\}$$

where K is normalising factor

$$K = \overline{K}\sqrt{2\pi}\,\Gamma\left(\frac{N+\delta+1}{2}\right) 2^{\frac{N+\delta+1}{2}} \tag{15}$$

$$\overline{K} = \sum_{d,a} \overline{K}_{d,a}$$

$$\overline{K}_{d,a} = \frac{\rho_{d,a}\, f(a,\, d)}{\sqrt{\widehat{Y}_{d,a}^{*T}\widehat{Y}_{d,a}^{*} + \rho_{d,a}^2}} \cdot$$

$$\cdot \left(Y^T Y + \epsilon + \left(\widehat{b}_{d,a}\rho_{d,a}\right)^2 - \frac{\left(\widehat{Y}_{d,a}^{*T} Y + \widehat{b}_{d,a}\rho_{d,a}^2\right)^2}{\widehat{Y}_{d,a}^{*T}\widehat{Y}_{d,a}^{*} + \rho_{d,a}^2}\right)^{-\frac{N+\delta+1}{2}}$$

The normalising factor must be enumerate in order that aposterior distribution fulfils basic feature of p(d)f $\int_* f(.) = 1$.

7.1.1 System Classification

The aposterior marginal distribution

$$f(d\,|Y_o,\, U) = \sum_a \int_{b^*, s^*} f(a,\, b,\, d,\, s\,|Y_o,\, U\,)\, d(\,b,\, s) \propto \sum_a \overline{K}_{d,a} \tag{16}$$

can serve for decision which order d (number of constituents) of models is the best one for the given data. We can consider the variable d with the MAP as the best choice of model structure or better exclude d-order models with too small AP. It can be useful for reduction of considered set of model orders with respect to assumption of the similar group of model orders for single regions at all patients.

7.1.2 Estimation of Precision Value s of Noise

Setting of prior pdf $f(s)$ is one of more difficult tasks. It can be adjusted roughly on the base of knowledge about measurement level. Another possibility is to obtain this distribution from pre-apriori processing of data records. It makes use of (14) respectively the marginal pdf $f(s\,|Y, U\,)$ and assumption of the same level of noise (see 6.2).

Bayes rule together with chain rule and data measured on region of upper limb D_i are used for setting pdf $\overline{f}(s)$ (D_i denotes all data for one region at one patient's limb). Data D_i are independent because they are obtained on different limbs. Then:

$$\overline{f}(s) \equiv f\,(s\,|D_1, D_2, \ldots, D_n\,) \quad \propto \quad f\,(D_1, D_2, \ldots, D_n\,|s\,)\; f(s) \tag{17}$$

$$
\begin{aligned}
&\propto \; f(D_n\,|s)\ldots f(D_2\,|s)\,\underbrace{f(D_1\,|s)\;f(s)}\\
&\propto \; f(D_n\,|s)\ldots \underbrace{f(D_2\,|s)\;f(s\,|D_1)}\\
&\propto \; f(D_n\,|s)\ldots f(s\,|D_1,D_2)\\
&\;\vdots
\end{aligned}
$$

The exact estimation with chosen group of models is practically impossible as the number of terms in likelihood function increases exponentially. Therefore approximation is necessary. The sum of gamma distribution $f(s\,|D_1,...,D_i)$ (arisen for the sake of discretisation of parameter a and various orders d of model) is replaced in each step of recursive estimation by one gamma distribution $\widehat{f}(s\,|D_1,...,D_i)$ with the same mean value and variance.

This method of noise setting allows us to make use of all sooner counted theoretical results. Other (and perhaps better) approximations would lead to unnecessarily complicated calculations.

7.2 Estimation of Time-Activity Curve

Evaluation of the whole pdf $f(x_t\,|y,\,u(\overline{t}))$ is unnecessary and complicated, mean value $E\left(x_t\,|y,\,u(\overline{t})\right)$ and variance $\operatorname{var}\left(x_t\,|y,\,u(\overline{t})\right)$ are sufficient results. We obtain it employing results of parameter estimation and calculus with pdfs:

$$
\begin{aligned}
E(X\,|Y,U) &= \sum_{d,a}\int_{b^*,s^*} X(a,d,b,U)f(a,d,b,s\,|Y,U)dbds && (18)\\
\operatorname{cov}(X\,|Y,U) &= E\left[(X-E(X\,|Y,U))(X-E(X\,|Y,U))^T\,\middle|\,Y,U\right]= && (19)\\
&= \sum_{d,a}\int_{b^*,s^*} X(a,d,b,U)X^T(a,d,b,U)f(a,d,b,s\,|Y,U)dbds\\
&\quad -E(X\,|Y,U)E(X\,|Y,U)^T
\end{aligned}
$$

Seeking variances $\operatorname{var}\left(x_t\,|y,\,u(\overline{t})\right)$ lie on diagonal of covariance matrix $\operatorname{cov}(X\,|Y,U)$.

The solution after simple re-arrangements is in following form:

$$
\begin{aligned}
E(X\,|Y,U) &= \frac{1}{\overline{\overline{K}}}\sum_{d,a} p_{d,a}\widehat{Y}^*_{d,a}\int_{b^*} b\mathcal{T}_b\left(\overline{b}_{d,a},\overline{H}_{d,a},N+\delta+1\right)db = && (20)\\
&= \frac{1}{\overline{\overline{K}}}\sum_{d,a} p_{d,a}\widehat{Y}^*_{d,a}E_{\mathcal{T}_b}(b) = \frac{1}{\overline{\overline{K}}}\sum p_{d,a}\widehat{Y}^*_{d,a}\overline{b}_{d,a}
\end{aligned}
$$

and

$$
\operatorname{cov}(X\,|Y,U) = \frac{1}{\overline{\overline{K}}}\sum_{d,a} p_{d,a}\widehat{Y}^*_{d,a}\widehat{Y}^{*T}_{d,a}\int_{b^*} b^2\mathcal{T}_b\left(\overline{b}_{d,a},\overline{H}_{d,a},N+\delta+1\right)db\;+ \qquad (21)
$$

$$
\begin{aligned}
& -E(X\,|Y,U)E(X\,|Y,U)^T = \\
= \;& \frac{1}{\overline{\overline{K}}}\sum_{d,a} p_{d,a}\widehat{Y}^*_{d,a}\widehat{Y}^{*T}_{d,a}\left(E^2_{\mathcal{T}_b}(b) + \mathrm{var}_{\mathcal{T}_b}(b)\right) - \\
& -E(X\,|Y,U)E(X\,|Y,U)^T = \\
= \;& \frac{1}{\overline{\overline{K}}}\sum_{d,a} p_{d,a}\widehat{Y}^*_{d,a}\widehat{Y}^{*T}_{d,a}\left(\overline{b}^2_{d,a} + \frac{(N+\delta+1)\overline{H}_{d,a}}{(N+\delta-1)}\right) - \\
& -E(X\,|Y,U)E(X\,|Y,U)^T
\end{aligned}
$$

where

$$
\begin{aligned}
z_{d,a} &= Y^TY + \left(\widehat{b}_{d,a}\rho_{d,a}\right)^2 + \epsilon - \frac{\left(\widehat{Y}^{*T}_{d,a}Y + \widehat{b}_{d,a}\rho^2_{d,a}\right)^2}{\widehat{Y}^{*T}_{d,a}\widehat{Y}^*_{d,a} + \rho^2_{d,a}} \\
\overline{b}_{d,a} &= \frac{\widehat{Y}^{*T}_{d,a}Y + \widehat{b}_{d,a}\rho^2_{d,a}}{\widehat{Y}^{*T}_{d,a}\widehat{Y}^*_{d,a} + \rho^2_{d,a}} \\
\overline{H}_{d,a} &= \frac{z_{d,a}}{(N+\delta+1)\left(\widehat{Y}^{*T}_{d,a}\widehat{Y}^*_{d,a} + \rho^2_{d,a}\right)} \\
p_{d,a} &= \frac{\rho_{d,a} f(a,d) z_{d,a}^{-\frac{N+\delta+1}{2}}}{\sqrt{\widehat{Y}^{*T}_{d,a}\widehat{Y}^*_{d,a} + \rho^2_{d,a}}}
\end{aligned}
$$

Remarks

> ***Definition of multivariate Student t-distribution and its main characteristics***. *A random vector v has a r-dimensional Student t-distribution with ν degrees of freedom, mean vector μ and precision matrix H^{-1} or more simply $V \sim \mathcal{T}_v(\mu, H, \nu)$ if it has a density function of the form*
>
> $$f(v) = \frac{\Gamma\left(\frac{\nu+r}{2}\right)\,|H|^{-\frac{1}{2}}}{\Gamma\left(\frac{\nu}{2}\right)(\nu\,\pi)^{\frac{r}{2}}}\left[1 + \frac{1}{\nu}(v-\mu)^T H^{-1}(v-\mu)\right]^{-\frac{\nu+r}{2}}$$
>
> *If $v \sim \mathcal{T}_v(\mu, H, \nu)$, then $E(v) = \mu$ and $\mathrm{cov}(v) = \frac{\nu H}{\nu-2}$. Univariate Student distribution is special case with $r = 1$.*

7.3 Estimation of Residence Time

Each triple of parameters $\{d, a, b\}$ and known input sequence $u(\overline{t})$ determine uniquely area under time-activity curve (residence time). It can be easy proved that area $S(x) = \sum_{i=1}^{\infty} x_i$ for model (4) and unit impuls at time $t = 1$ is convergent infinite series with total sum

$$S(d,a,b) = \sum_{i=1}^{\infty} x_i = \frac{b}{(1-a)^d} \tag{22}$$

Mean value and variance of estimated residence time can be then determined likewise as in previous subsection.

7.4 Optimization of Measurement Moments

Impracticable full time measurement forces us to occupy with the question how many times and when to measure. This problem have to be solved iteratively to obtain required results with the smallest number of measurements. Section provides theoretical background for decision in which fix number of moments to measure output to minimize error of residence time estimate.

Consider $\overline{p}$ measured patients limbs on single ROI with series of measurement Y_p in identical N moments, $dim(Y_p) = N$ and known U_p $(D_p = (Y_p, U_p)$. The aim is to decide in which M moments $(0 < M < N)$ from N measured ones is best to record output signal to minimize error of residence time estimate on basis of data from these $\overline{p}$ extremities.

Using formalism established in decision-making theory (see section 4) $\mathcal{Q} \equiv \left(\mathcal{P} = \{D_1, \ldots, D_{\overline{p}}\}; a = \left(\widehat{S}_1, \ldots, \widehat{S}_{\overline{p}}, m\right); \mathcal{F} = S_1, \ldots, S_p\right)$ where $\widehat{S}_p$ is point estimate of real residence time S_p on single ROI of p extremity and m is decision when to measure. If we select quadratic loss function $\mathcal{Z} \equiv \sum_p \left(S_p - \widehat{S}_p\right)^2$ then we find

$$\left(m^o, \widehat{S}_p^o\right) = \arg\min_{m, \widehat{S}_p} E\left(\sum_p \left(S_p - \widehat{S}_p\right)^2\right) \tag{23}$$

where solution is

$$\widehat{S}_p^o = E\left(S_p \,|m, D_p\right) \tag{24}$$

$$m^o = \arg\min_m \sum_p \mathrm{var}(S_p \,|m, D_p) \tag{25}$$

The conclusion is reasonable and expected. The best point estimate of the residence time is its aposterior mean value. The moments of measurements have to be selected so the sum of aposterior variances of area estimates over patients' extremities is minimized.

8 Tuning and Tests

The formed theory shapes the basis of software tool written meanwhile in Matlab. The software was tested on simulated data first and then tuned on real data to be prepared for practical treatment.

Tests on Simulated Data

Simple experiments on simulated data were performed to verify the correctness of tool results. The data was generated by assumed model (4) with known values of parameters. The evaluation results to following important aspects.

Noise level influences significantly the result of estimation. It is needful to distinguish noise generated in simulation and noise set in prior information. Bigger generated noise make worse identification naturally. Good results were obtained, when the deviation of noise was one degree smaller than deterministic data. Other problem makes wrong set noise in prior information. In spite of that the generated noise is sufficiently small, for apriori set big noise the fitting is not so successful. Therefore it is better to adjust smaller noise in prior information at the beginning if we know nothing about it.

If we would omit noise disturbance and utilize e.g. the well known least squares estimation method instead of designed estimator, we would need many measurements even so the estimate will not be unbiased. The designed estimator is unbiased but process of estimation is in our case limited by ***number of measurements***. With increasing number the estimation makes better naturally but we are constrained by real abilities. The reasonable lower limit of measurement moments for sufficient estimation is equal to number of parameters. It is necessary to reckon with deterioration of estimation when the number of measurements sinks under this limit. In spite of this fact the estimates from demanded 2 measurements is satisfactory.

The biggest problem comes with ***estimation of noise***. Convergence of noise estimate is slower than by other parameters. The noise does not catch to converge in estimation process with a few number measurements (for better estimation is necessary to repeat calculation more times). It results in conclusion that the prior information of noise have to be adjusted sufficiently well before employing estimator in practice.

All aspects are bound each other and this calls for a respect.

Tuning on Real Data

The acquisition and preprocessing of real data is described in section 3. Number of measurements performed on patients' extremities varies between 2 and 4. Data of patients recorded only twice was not employed in tuning phase.

The first task is choice of sample period (period of discretisation). The lower bound of period is 1 minute because real data are obtained from frames of 60 seconds, but this sampling is unnecessary fine. Done experiments with various reasonable sample period exposed negligible influence of time-activity curve estimates on sample period. Sample period was fixed to 5 minutes.

The prior distribution on parameters a, d is chosen so the average value of maximal uptake is 10% and the latest time of uptake is 5 hours.

Other important task is setting of prior distribution $f(s)$ that represents characteristics of noise. It is obtained from pre-apriori processing of data records suggested in 7.1.2. The results of noise estimation are shown in Fig. 2.

The last task performed in phase of tuning is classification described in 7.1.1. It serves for the determination which orders of models are reasonable and which can be omitted. Reason for it is reduction of assumed set of model orders and from it following enhancement of computational efficiency. The results are summarized in histograms as average of classification results over extremities in Fig.

Figure 2: Results of pre-apriori estimation of $f(s)$ together with adequate $f(r)$ ($r = \frac{1}{s}$) from data of 16 extremities for single regions.

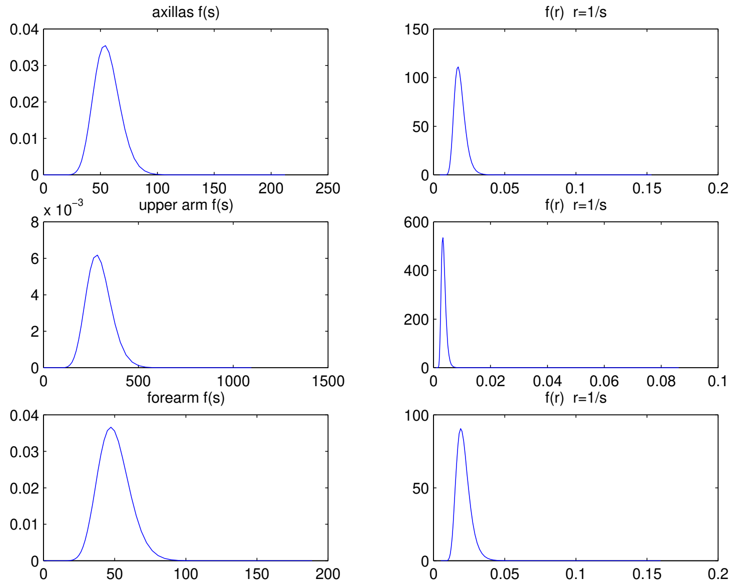

3. It demonstrates that chain of maximally 6 simple identical compartmental models is adequately long. On the basis of results bounds of parameter d is fixed to $1 \leq d \leq 5$ for regions of forearm and $2 \leq d \leq 4$ for region of axillas and upper arm.

9 Results of Practical Treatment

Quality of proposed dynamic model was verified on practical data . The results of estimation are demonstrated here on 2 limbs in Fig. 4. It employs 3 measurements in the former and 4 measurements in the latter case.

The influence of measurement moments on estimation of residence time is expressed in Tables 1, 2, 3. Residence time is estimated from all measurements first and then from all possible combination of 2 measurements. Values served for optimization of 2 moments of measurement. Task of optimization described in section 7.4 have to be little modified because it is difficult to ensure identical measurement moments by all patients. Instead of point moments we can consider time intervals and the result is the same as (**??**).

Results of optimization for single regions with defined time intervals

Table 1: Residence time S estimated from various data on region of axillas.

Nr	Measur. moments	Limb	Used measurements: all		[1 2]		[1 3]		[2 3]		[1 4]		[2 4]		[3 4]	
			$E(S)$	$\sigma(S)$	$E(S)$	$\sigma(S)$	$E(S)$	$\sigma(S)$	$E(S)$	$\sigma(S)$	$E(S)$	$\sigma(S)$	$E(S)$	$\sigma(S)$	$E(S)$	$\sigma(S)$
1	[38 152 204]	left	1369	457.8	1948	1377	2067	962.9	1466	386.2						
		right	2202	759.4	1136	776.7	1334	714.5	1579	640.8						
2	[38 76 126 203]	left	143.7	86.69	254.2	243.7	145.8	120.9	151.1	120.3	139.3	76.38	139.3	81.24	144.5	80.40
		right	991.3	184.4	868.1	754.3	676.3	444.5	648.7	428.4	794.3	260.8	782.8	262.5	920.3	387.5
3	[30 136 201]	left	2434	200.6	1319	422.6	1925	367.0	2604	1011						
		right	965.5	445.4	683.2	417.0	782.7	373.3	955.4	408.9						
4	[40 140 195]	left	1115	187.1	785.8	296.8	976.1	230.6	1183	273.3						
		right	697.2	254.6	574.8	277.3	629.1	230.9	794.9	327.0						
5	[40 95 140 195]	left	2141	95.29	2982	1282	2148	542.5	3597	1799	2536	1450	2465	649.3	2292	464.9
		right	2282	90.70	3159	1338	2279	568.1	3808	1878	2638	1478	2616	687.5	2435	490.5
6	[30 57 116 177]	left	3302	519.1	1314	1088	1321	1087	1639	1088	1482	965.1	1989	1121	1860	888.6
		right	2723	517.3	1350	1125	1565	1133	1412	924.1	1764	1036	1733	863.4	1802	868.3
7	[35 78 130 220]	left	2311	963.0	1225	1018	1251	502.5	1895	1023	1928	802.1	2944	1380	2660	980.0
		right	3015	227.6	2694	1869	2830	1624	2727	1555	2333	756.4	2251	710.5	2182	612.7
8	[32 141 203]	left	2009	155.4	1306	475.6	1644	303.1	1807	553.3						
		right	1651	98.65	1052	243.0	1521	149.9	1708	521.3						

Table 2: Residence time S estimated from various data on region of upper arm.

Nr	Measur. moments	Limb	Used measurements: all		[1 2]		[1 3]		[2 3]		[1 4]		[2 4]		[3 4]	
			$E(S)$	$\sigma(S)$	$E(S)$	$\sigma(S)$	$E(S)$	$\sigma(S)$	$E(S)$	$\sigma(S)$	$E(S)$	$\sigma(S)$	$E(S)$	$\sigma(S)$	$E(S)$	$\sigma(S)$
1	[38 152 204]	left	138.83	26.34	124.1	35.30	140.8	26.05	136.6	27.78						
		right	815.9	82.13	509.1	142.7	610.1	120.0	679.6	112.0						
2	[38 76 126 203]	left	397.0	67.63	246.5	101.1	258.3	84.30	279.6	83.02	329.4	48.25	356.1	62.48	360.0	59.09
		right	212.6	22.07	223.0	113.5	153.2	35.44	148.5	31.97	219.0	25.23	214.0	28.72	220.2	41.90
3	[30 136 201]	left	633.4	41.23	468.2	113.5	582.3	74.42	613.2	106.0						
		right	1249	20.56	1106	187.4	1201	48.14	1144	116.2						
4	[40 140 195]	left	149.9	34.35	128.2	38.77	149.3	32.22	149.4	31.54						
		right	170.0	39.98	147.6	45.55	166.3	36.73	164.6	33.77						
5	[40 95 140 195]	left	187.7	12.03	143.4	25.68	162.2	16.53	163.6	29.89	215.3	16.62	195.3	26.15	200.7	38.06
		right	141.1	13.87	113.7	31.92	110.0	14.48	113.3	21.16	168.3	17.99	159.9	29.06	156.2	32.69
6	[30 57 116 177]	left	76.34	23.97	63.43	51.06	77.50	34.07	83.04	33.63	72.13	21.69	70.82	24.05	75.38	22.48
		right	347.7	48.87	239.5	134.8	245.6	93.19	231.1	81.16	300.8	73.10	299.5	69.11	300.9	60.58
7	[35 78 130 220]	left	237.6	35.63	128.1	67.36	167.6	58.04	172.3	50.42	216.7	37.96	210.0	38.50	209.4	38.23
		right	339.6	38.14	206.5	102.6	211.8	61.77	222.9	67.77	318.9	44.43	318.0	56.04	308.3	51.76
8	[32 141 203]	left	567.3	38.93	423.7	98.79	528.3	63.31	549.0	92.62						
		right	1093	49.27	971.1	296.2	959.4	152.7	929.7	135.6						

Table 3: Residence time S estimated from various data on region of forearm.

Nr	Measur. moments	Limb	Used measurements													
			all		[1 2]		[1 3]		[2 3]		[1 4]		[2 4]		[3 4]	
			$E(S)$	$\sigma(S)$	$E(S)$	$\sigma(S)$	$E(S)$	$\sigma(S)$	$E(S)$	$\sigma(S)$	$E(S)$	$\sigma(S)$	$E(S)$	$\sigma(S)$	$E(S)$	$\sigma(S)$
1	[38 152 204]	left	95.49	32.92	94.70	44.44	84.14	43.35	1773	1809						
		right	193.4	52.85	151.8	54.68	210.8	53.38	500.8	1056						
2	[38 76 126 203]	left	475.4	97.83	356.9	170.0	339.5	112.4	363.0	128.7	441.4	71.96	473.1	104.1	468.6	103.8
		right	77.92	24.76	86.38	57.37	78.86	34.21	100.0	53.63	79.06	34.79	100.4	58.75	550.6	553.8
3	[30 136 201]	left	93.38	36.34	75.34	39.09	111.3	50.12	634.5	783.5						
		right	1339	65.99	908.7	109.5	1471	74.51	1378	304.0						
4	[40 140 195]	left	117.2	40.39	100.3	48.72	116.6	49.23	791.4	1086						
		right	65.82	30.93	61.00	37.36	61.84	39.12	904.5	961.7						
5	[40 95 140 195]	left	320.2	39.91	288.6	134.6	247.8	44.89	315.1	88.96	347.2	43.11	332.8	70.14	336.3	109.9
		right	255.3	69.32	195.4	102.2	182.8	67.99	208.6	78.74	254.9	61.00	245.1	64.79	270.4	230.4
6	[30 57 116 177]	left	60.21	30.71	72.68	78.33	66.08	43.91	64.67	40.42	50.61	36.98	49.02	32.68	348.4	346.3
		right	85.62	36.91	119.2	106.6	77.97	47.14	81.34	42.46	80.50	43.70	81.87	38.46	314.0	341.8
7	[35 78 130 220]	left	112.4	36.69	101.8	66.08	99.3	41.95	123.4	61.77	129.8	54.17	130.9	64.43	604.0	738.1
		right	77.91	32.08	70.89	51.06	70.40	36.89	96.50	61.03	91.67	49.07	96.72	60.85	569.1	637.2
8	[32 141 203]	left	153.0	30.18	135.1	33.47	190.1	54.94	717.7	1099						
		right	135.8	39.15	112.4	42.20	163.6	52.93	685.1	1031						

Figure 3: The average of classification results over16 extremities for single regions. It describes suitability of model orders (x axis-order).

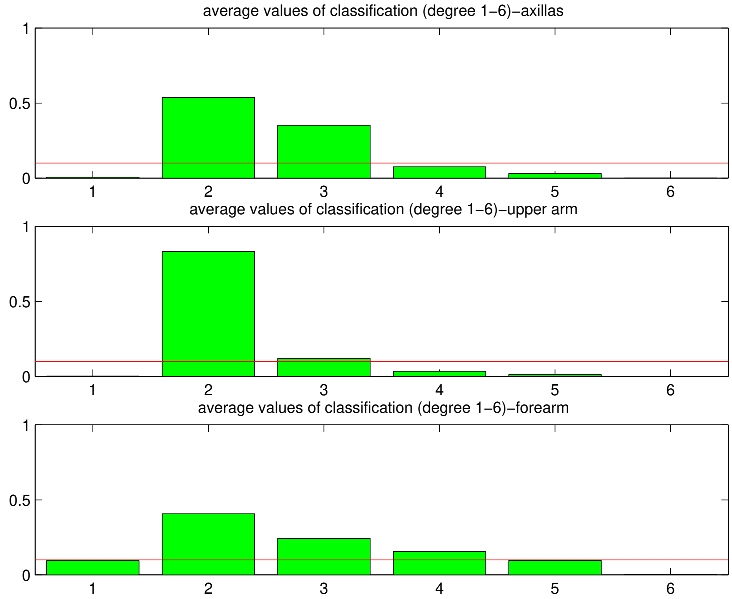

Interval	Range of interval (mins)
I_1	$\langle 30, 50\rangle$
I_2	$\langle 55, 95\rangle$
I_3	$\langle 115, 155\rangle$
I_4	$\langle 175, 220\rangle$

are summarized in this table

Region	Ordered combination of intervals(the best $\rightarrow$ the worst)
axillas	$\{I_3, I_4\}$ $\{I_2, I_4\}$ $\{I_1, I_4\}$ $\{I_1, I_3\}$ $\{I_2, I_3\}$
upper arm	$\{I_1, I_4\}$ $\{I_2, I_4\}$ $\{I_3, I_4\}$ $\{I_1, I_3\}$ $\{I_2, I_3\}$
forearm	$\{I_1, I_4\}$ $\{I_1, I_3\}$ $\{I_2, I_4\}$ $\{I_2, I_3\}$ $\{I_3, I_4\}$

It shows that for more distant place from injection the later data are important. It holds good the late measurement is important for all regions. If it is not known observation on which region are suitable for assessing disease compromise of choice of time intervals has to be made. The combination $\{I_1, I_4\}$ looks as good one. The exploration of estimated time-activity curves is possibility how to verify precede conclusion. One example is demonstrated in Fig. 5.

Figure 4: Two examples of estimation of time-activity curves and residence times from all data. 3 subgraphs correspond to regions of interests. Stars denotes measured data, bold solid line estimated mean value of time activity curve, and doted lines the shape (mean value ±standard deviation). Mean value and deviation of estimated residence time is written out on the right of graphs.

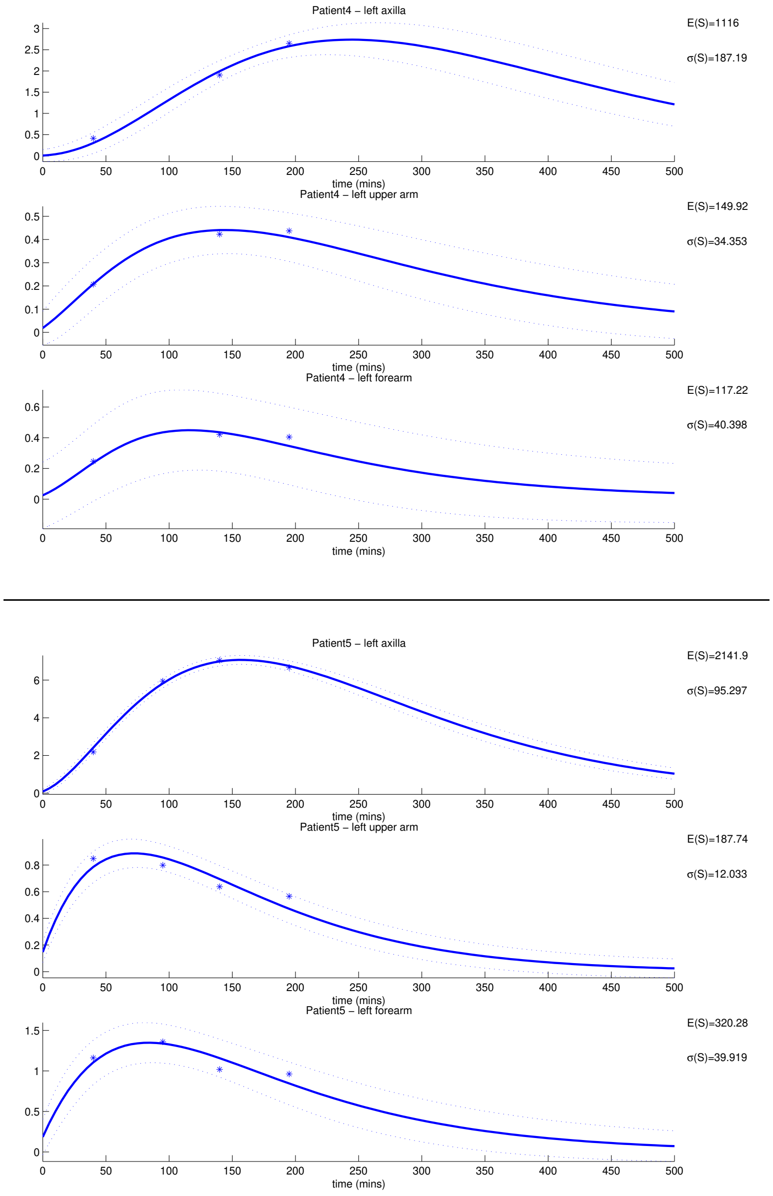

Figure 5: Example of time activity curves and residence times estimation from 2 measurements. All combination are presented.(+ denotes data not used for estimation)

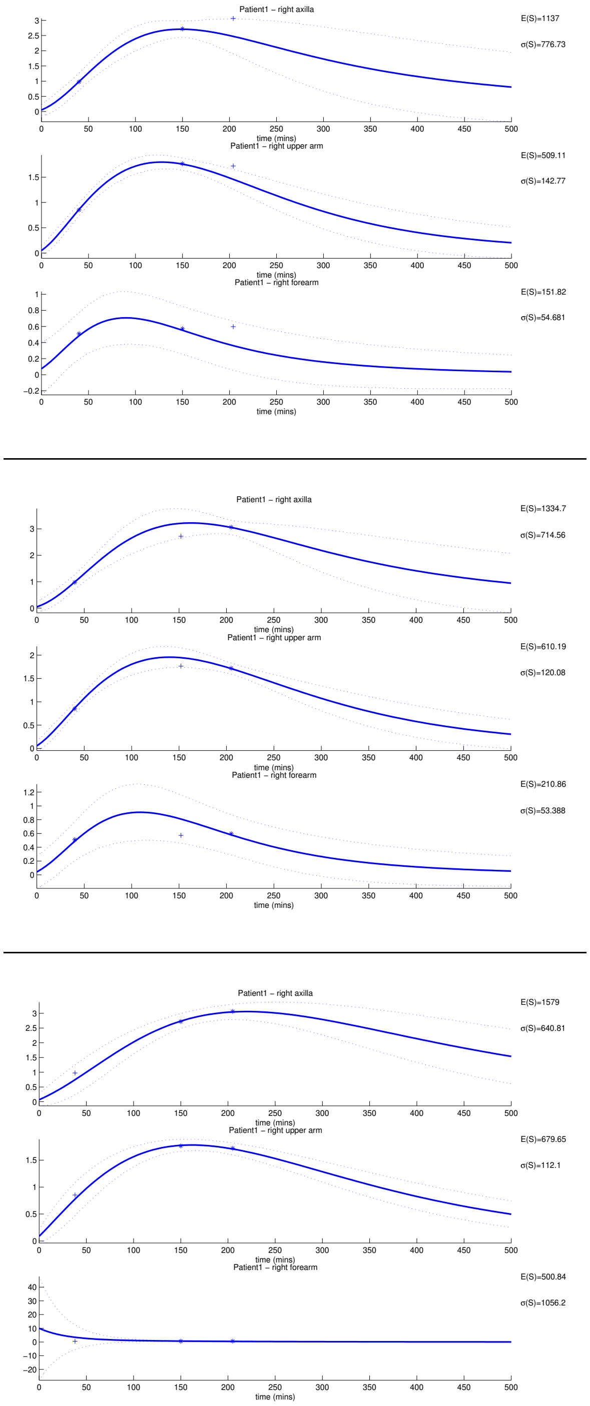

Figure 6: Comparison of time-activity curves (respectively their shapes) on left and right limb.

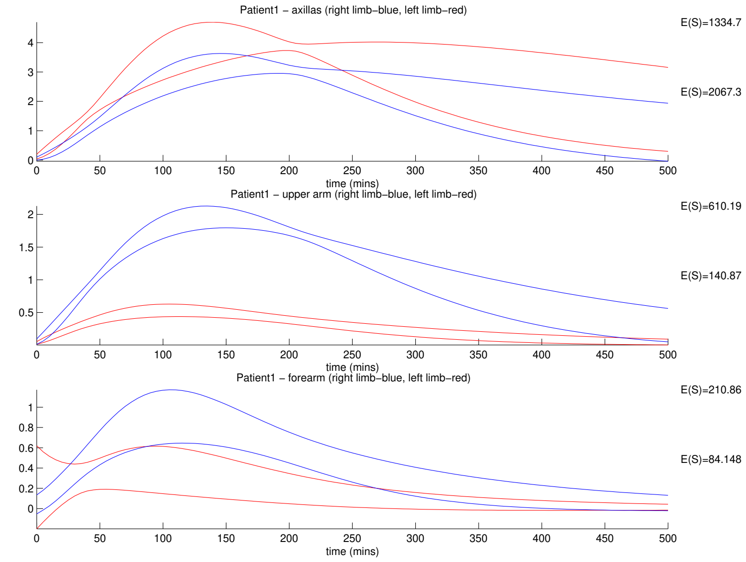

10 Discussion

Actual state of investigation does not permit to select only one region of interests for evaluation of the disease. Therefore time-activity curves together with residence times are evaluated for each region. The advantage of more computing is possibility to determine the position of lymph tapering or blocking easily. It is evident from combination of time-activity curves in each region.

Time-activity curves are the most important results. They can be used for additional processing. An example is to utilize this curves for obtaining maximal uptake instead of uptake in concrete time moments. The curves lend itself to comparison of left and right limb or one limb before and after treatment because there exists symmetricity in lymphatic morphology of limbs. On the contrary lymph morphology of various patients can differ. Comparison of curve shapes with respect how they overlap is found as good way (Fig. 6).

The problems can appear at estimation when the signal is too small. This case happens at estimation on region where no nodes exist and the limb is healthy. Consequently the best region for estimation and following evaluation appears such area where all people have nodes — region of axillas. Only exception are patients after surgical removed axillas nodes.

We have to emphasize that 3 measurements would be optimal compromise for estimation. Demanded only 2 frames should be obtained in times about 50 and 180 minutes to ensure first-quality results. If one region turns out as dominant, moments of measurement should be adjust.

Estimate of the residence time has the same characteristics and the same conclusions hold good for it as for time-activity curve. Its advantage is that it attempts to quantify the state of lymphatic system. The results in problematic cases is again bad – sometimes the estimated deviation is bigger than mean value.

The detailed study connecting these estimates with assessment of the disease grade was not performed yet. The main present-day problem is the lack and quality of data.

Paper describes one of possibilities of system identification employing for evaluation of lymphedema on upper limbs. In spite of the method is defined precisely, there exist still open problems (how to continue or alternative approaches):

- One group of problems refers to a preprocessing of data. This group includes questions, if it is useful to correct data for decay of radionuclide, if to correct data for tissue absorption then how.
- Seeking of suitable regions of interests for assessing of the disease.
- Creation of model with Poisson distribution. It would describe problem better but bring solution troubles.
- Modeling of the transportation of lymph in the limb as a whole with spatial relations. It is more complicated but can bring further information.

11 Conclusion

The Bayesian system identification from sparse measurements has been addressed. It has served for description of lymphatic system behaviour on local regions (accumulation of radioactive tracer) of upper limb during lymphoscintigraphic procedure. The behaviour on single regions has been modeled independently be means of chain of identical compartmental models. This practical example has verified that not usual identification from sparse measurements is practically feasible.

The main purpose of identification was reconstruction of the whole time-activity curves on individual regions from a few measurements. Designed estimator counts besides curves also residence times. The curves and residence times are final results of outlined study but they will be used for additional processing by doctors.

The evaluation results indicate adequacy of the adopted model and encourage us to follow the direction. Meantime the tool is suitable for judgment of (in)significance of differences between both limbs. The followed task will be concerned study of quantitative relationships between disease staging and measurements.

The proposed approach is progress in processing of lymphoscintigraphic data. It ranks among first attempts with utilization of modeling in this field.

References

[1] Fruhling, J.G., Bourgeois, P., 1983. Axillary lymphoscintigraphy: current status in the treatment of breast cancer. In: *CRC Critical Reviews in Oncology/Hematology* 1, 1-20.

[2] Heřmanská, J., Kárný, M., Jirsa, L., Němec, J., 1998. Evaluation of biophysical quantities related to the treatment of thyroid diseases. In: *Quantitative Image Analysis in Functional Scintigraphic Imaging*, GAMAMED, Prag, September 1998, 39-42.

[3] Kárný, M., Nagy, I., 1999. Dynamic Bayesian decision-making.

[4] Peterka, V., 1981. Bayesian approach to system identification. In: *Trends and Progress in System Identification*, P. Eykhoff, Ed., Pergamon Press, Oxford, 239-304.

[5] Verlooy, H., Biscompte, J.P., Nieuborg, L., Drent, P., Schiepers, C., Mortelmans, L., De Roo, M., 1997. Noninvasive evaluation of lympho-venous anastomosis in upper limb lymphedema.. In: *The European Journal of Lymphology*, vol. 6, 27-33.

[6] Weissleder, H., Weissleder,M., 1988. Lymphedema: evaluation of qualitative and quantitative lymphoscintigraphy in 238 patients. In: *Radiology*, vol. 167, 729-735.